Institute of Chemical Technology, Prague
Department of Computing and Control Engineering

BIOMEDICAL SIGNAL AND IMAGE PROCESSING

Ph.D. Thesis Synopsis

Victor Musoko

Supervisor: Prof. Ing. Aleš Procházka, CSc.

Specialization: Technical Cybernetics

Prague **July 2005**

Abstract

The main goal of the thesis is to show the de-noising algorithms based upon the discrete wavelet transform (DWT) that can be applied successfully to enhance noisy multidimensional magnetic resonance (MR) data sets i.e two-dimensional (2-D) image slices and three-dimensional (3-D) image volumes. Noise removal or de-noising is an important task in image processing used to recover a signal that has been corrupted by noise. Random noise that is present in MR images is generated by electronic components in the instrumentation. The thesis present both 2-D image decomposition, thresholding and reconstruction and the 3-D de-noising of MR image volumes using the DWT as a new approach which can be used in the processing of biomedical images. A novel use of the complex wavelet transform for the study and application in the de-noising of MR images is presented in the main part of the thesis. Segmentation of image textures using a watershed transform and a wavelet based feature extraction for classification of image textures by a competitive neural network will be shown.

Further topic of interest to be presented in the thesis is the visualization of 2-D MR slices and 3-D image volumes using some MATLAB functions. This makes it possible to visualize images without the need of special glasses especially for 3-D image volumes or using special expensive software programs which will need some bit of expertise. The application of the proposed algorithms is mainly in the area of magnetic resonance imaging (MRI) as an imaging technique used primarily in medical field to produce high quality images of the soft tissues of the human body. An insight to the visualization of MRI data sets i.e. 2-D image slices or 3-D image volumes is of paramount importance to the medical doctors.

The thesis presents the theory of the fundamental mathematical tools (discrete Fourier transform (DFT) and DWT) that are used for the analysis and processing of biomedical images. DWT plays an increasingly important role in the de-noising of MR images. 3-D digital image processing, and in particular 3-D DWT, is a rapidly developing research area with applications in many scientific fields such as biomedicine, seismology, remote sensing, material science, etc. The 3-D DWT algorithms are implemented as an extension of the existing 2-D algorithms. The performance of the de-noising algorithms are quantitatively assessed using different criteria namely the mean square error (MSE), peak signal-to-noise ratio (PSNR) and the visual appearance. The results are discussed in accordance to the type of noise and wavelets implemented. The properties of wavelets make them special in that they have a good time and frequency localization which make them ideal for the processing of non-stationary signals like the biomedical signals (EEG, ECG,..) and images (MR). The traditional Fourier transform only provides the spectral information of a signal and thus it is not suitable for the analysis of non-stationary signals.

A novel complex wavelet transform (CWT) which was introduced by Dr. Nick Kingsbury of Cambridge University is analyzed and implemented in the main part of the thesis. The description of the dual tree implementation of CWT is followed by its analysis and discussions devoted to its advantages over the classical wavelet transform. This enhanced transform is then applied to MRI data analysis. Experimental results show that complex wavelet de-noising algorithm can powerfully enhance the PSNR in noisy MRI data sets.

The further part of the thesis devoted to the description of basic principles of a watershed transform for segmentation of MR images. After its verification for simulated textures it is used for segmentation of a human knee MR image. The anatomical regions of the knee which includes the muscle, bone and tissue can be easily distinguished by this algorithm. Segmentation is an important field in medical applications and can be used for disease diagnosis e.g. detecting brain tumor cells.

Texture analysis of artificial textures based on image wavelet decomposition is considered as a pre-processing method for the classification of the textures. The wavelet features are obtained by using the mean or the standard deviations of the wavelet coefficients. For the classification of the textures these feature vectors form the inputs to a competitive neural network. The work also presents own algorithms for class boundaries evaluation. Texture analysis is used in a variety of applications, including remote sensing, satellite imaging, medical image processing, etc.

Finally, I conclude and give suggestions for future research work. The thesis also gives a review of the de-noising and visualization of biomedical images on the web using the Matlab Web Server (MWS).

Keywords

Time-Frequency and Time-Scale Signal Analysis, Discrete Wavelet Transform, Complex Wavelet Transform, Image De-noising, Biomedical Image Processing, Watershed Algorithm, Segmentation, Feature Extraction, Image Visualization

Abstrakt

Cílem disertační práce je návrh a analýza algoritmů založených na aplikaci diskrétní wavelet transformace (DWT) pro potlačení rušivých složek a zvýraznění vícerozměrných souborů dat. Aplikační část práce je přitom věnovaná obrazům magnetické resonance (MR) a jejich zpracování v případě dvourozměrné (2-D) vrstvy a třírozměrného (3-D) obrazu. Potlačování rušivých složek je důležitou úlohou zpracování obrazů pro oddělení signálu od šumu. Šum obrazů magnetické resonance se přitom skládá z náhodných signálů generovaných elektronickými komponentami systému. Práce presentuje jak dvourozměrnou dekompozici, prahování a následující rekonstrukci obrazů tak i potlačování rušivých složek ve třírozměrném prostoru s využitím DWT jako nové metody, která muže být aplikována na zpracování biomedicínských obrazů. Nová uplatnění komplexní wavelet transformace implementující duální strom (DT CWT) pro studie a aplikace na potlačování rušivých složek obrazů MR je prezentována v hlavní části práce. Segmentace obrazových textur pomocí rozvoďové (watershed) transformace a jejich klasifikace pomocí vzorů získaných z wavelet transformace tvoří další část práce. Vzory jsou přitom využity jako vstupy do samoorganizující se neuronovou síť.

Dalším tématem práce je vizualizace 2-D vrstev a 3-D obrazů pomoci systému MATLAB. Tato cesta umožňuje zobrazit obraz bez používání speciálních technických pomůcek nutných pro vizualizaci 3-D obrazů nebo používání speciálních a často velice složitých komerčních programů. Aplikace navržených algoritmů je zejména v oblasti zobrazování výsledků získaných pomocí magnetické rezonance (MRI) jako moderní vyšetřovací metody používané hlavně v lékařské praxi pro získávání vysoce kvalitních obrazů vnitřních orgánů lidského těla. Vizualizace sad MRI dat je přitom důležitá zejména pro lékařskou diagnostiku.

Práce prezentuje v teoretické části základní matematické metody analýzy a zpracování biomedicínských obrazů zahrnující diskrétní Fourierovu transformaci (DFT) a zejména diskrétní wavelet transformaci (DWT), která se stále významněji uplatňuje při analýze a potlačování rušivých složek signálů. Práce přitom zahrnuje i třírozměrné zpracování obrazů pomocí DWT (3-D DWT), které je z algoritmického hlediska zobecněním metod dvourozměrných a tvoří výzkumnou oblast, který má aplikace v různých vědních oborech včetně biomedicíny, seismologie, analýzy životního prostředí ap. Výsledky numerických experimentů jsou dále hodnoceny z hlediska kvality obrazů na základě vyhodnocování středních kvadratických chyb (MSE) a maximálních hodnot poměrů signál - šum (PSNR)

s ohledem na typ šumu a implementované wavelet funkce. Při rozborech jsou přitom využité vlastnosti wavelet funkcí zahrnující zejména jejich dobrou časovou a frekvenční lokalizaci. Tato vlastnost je zejména důležitá pro zpracování nestacionárních signálů, které se vyskytují v biomedicíně a zahrnují EEG a EKG signály a dále biomedicínské obrazy. V práci je ukázáno i porovnání s klasickou Fourierovou transformací, která poskytuje jen spektrální informace o celém signálu a neumožňuje časovou lokalizaci nestacionárních komponent pozorovaných dat.

Komplexní wavelet transformace implementující duální strom jako nová transformace, kterou navrhl Dr. Nick Kingsbury z Cambridge university, je analyzována a implementována v hlavní části práce. Práce popisuje teorii této transformace s následující analýzou a diskusí jejích výhod ve srovnání s klasickou WT. Tato rozšířená transformace je dále aplikována na analýzu a vyhodnocování MRI dat. Experimentální výsledky ukazují že potlačování rušivých složek signálů pomocí CWT metody výrazně zvyšuje hodnoty PSNR reálných MRI souborů.

Další část práce je věnována popisu základních principů rozvoďové transformace použité pro segmentaci MR obrazů. Po jejím ověření na simulovaných datech jsou navržené algoritmy následně užity pro segmentaci MR obrazu kolena. Anatomické oblasti kolena, které zahrnují svaly, kosti a tkáně jsou snadno touto transformací odlišeny. Segmentace je přitom velmi důležitá i v dalších biomedicínských aplikacích a může být používána k diagnóze nemocí například při detekování mozkových nádorů.

Analýza umělých textur pomocí wavelet dekompozice obrazu je v práce představena jako metoda pro předzpracování obrazů z hlediska jejich následné klasifikace. Vlastnosti obrazových segmentů jsou přitom získány ze středních hodnot nebo směrodatných odchylek wavelet koeficientů. Tyto vzory tvoří sloupcové vektory pro vstup do samoorganizující neuronové sítě z hlediska jejich klasifikace. Navržené algoritmy zahrnují rovněž výpočet hranic jednotlivých tříd. Analýza textur nachází přitom uplatnění v různých aplikacích, které zahrnují dálkové snímání, družicová pozorování, zpracování obrazů a další.

V závěru práce jsou formulovány návrhy pro další výzkumnou práci v uvedené oblasti. Disertační práce poskytuje navíc i popis užití Matlab Web Server (MWS) pro vzdálené zpracování a vizualizaci biomedicínských obrazů přes webové rozhraní.

Klíčová slova

Diskrétní wavelet transformace - dekompozice a rekonstrukce obrazů - komplexní wavelet transformace - potlačování rušivých složek obrazů - zpracování biomedicínských dat - segmentace obrazů - specifikace vlastností - klasifikace - umělé neuronové sítě - vizualizace

Introduction

Image processing can be defined as the manipulation of an image for the purpose of either extracting information from the image or producing an alternative representation of the image. There are numerous specific motivations for image processing but many fall into the following categories: (i) to remove unwanted signal components that are corrupting the image and (ii) to extract information by rendering it in a more obvious or more useful form.

Noise in MR images consists of random signals that do not come from the tissues but from other sources in the machine and environment that do not contribute to the tissue differentiation. The noise of an image gives it a grainy appearance and mainly the noise is evenly spread and more uniform. It is often desirable to process it to enhance the visibility of certain features such as the edges of a tumor. There are many advanced methods of image processing involving techniques that include the traditional Fourier transform and the wavelet transform. Recently a dual tree complex wavelet transform (DT CWT) was developed and has added advantages over classical methods, these include shift invariance and improved directionality.

In the thesis, wavelet transform is used for multi-scale signal analysis, the de-noising algorithms apply a chosen wavelet on wavelet decomposition for the reconstruction of MRI images. Experiments are done on 2-D and 3-D MRI data sets. Each part starts with algorithms for the 2-D case (image slices) and then continues with generalizing the algorithms to handle the 3-D case (image volumes). 3-D DWT algorithm is implemented as an extension of the existing two-dimensional (2-D) algorithms. The performance of the de-noising algorithms are quantitatively assessed using different criteria namely the PSNR, MSE and the visual appearance.

An efficient and accurate watershed algorithm was developed by Vincent and Soille [23] who used an immersion based approach to calculate the watershed lines. The method is tested on the segmentation of simulated and MR images. Texture is scale dependent, therefore a multi-scale or multi-resolution analysis of an image is required for texture analysis. We have proposed the use of image wavelet decomposition [4, 20], using wavelet coefficients at selected levels to describe image features. Classification of image segments into a given number of classes using segment features is done by a competitive neural network. An example of the classification of simulated image textures is shown.

The main objectives of the thesis can be summarized as follows:

- visualization and presentation of three-dimensional 3-D models
- presentation of the DWT de-noising algorithms that are applied successfully to enhance the noisy MR data sets (2-D image slices and 3-D image volumes)
- application of DT CWT in the analysis and de-noising of MR biomedical images
- introductory principle of the watershed algorithm for image texture segmentation
- classification of image textures using a competitive neural network

Biomedical Image Visualization

MRI acquisition of magnetic resonance images helps the biomedical engineers to fully analyze different aspects of the brain thereby reducing the need for surgery. With appropriate image analysis techniques, a biomedical engineer can use one small set of MR images and manipulate them to analyze some interesting facets of the brain. To load MR images of the brain into MATLAB and perform the necessary image analysis the task will require us to display all of the frames in one figure as a sequence of images. The cross sectional view of MR images as a 2-D representation of the slices is shown in Fig. 1

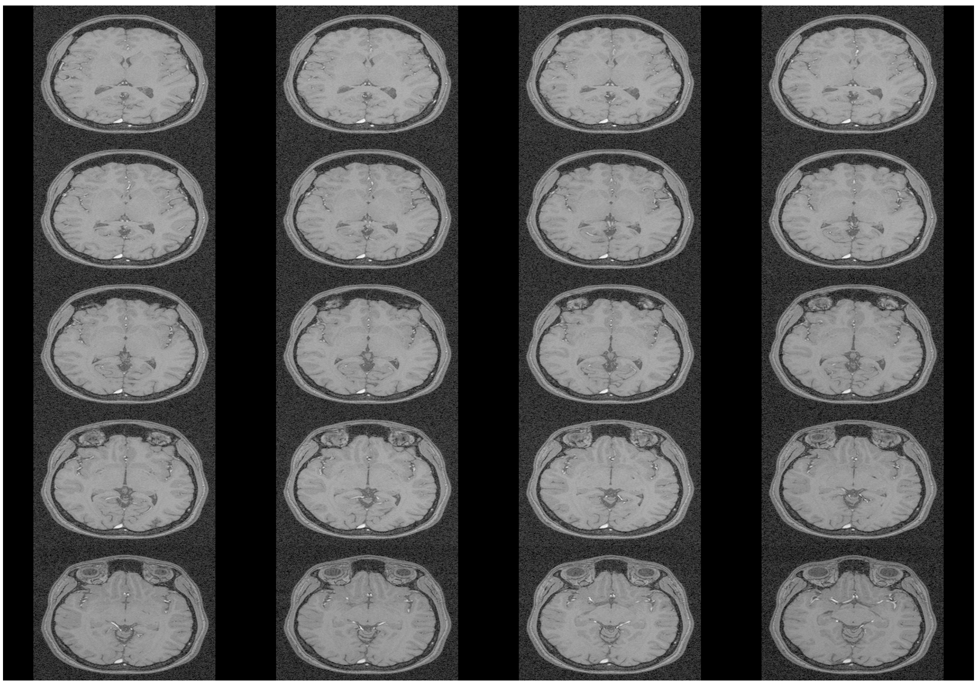

FIGURE 1. A sequence of MR image slices

Three dimensional imaging [3] is now widely available and used often to aid in the comprehension and application of volumetric data to diagnosis, planning and therapy. Especially in clinical neurosurgery [6] 3-D visualization would benefit the planning and surgical treatment immensely. Models of the image data can be visualized by volume or contour surface rendering and can yield quantitative information.

A multimodal visualization MATLAB code was tested with the MR image data sets. To reduce computational time of 3-D reconstruction of the MR image slices a volume of interest (VOI) of size $100 \times 400 \times 70$ voxels was extracted and rendered into 3-D model producing an excellent 3-D image subvolume (Fig. 2).

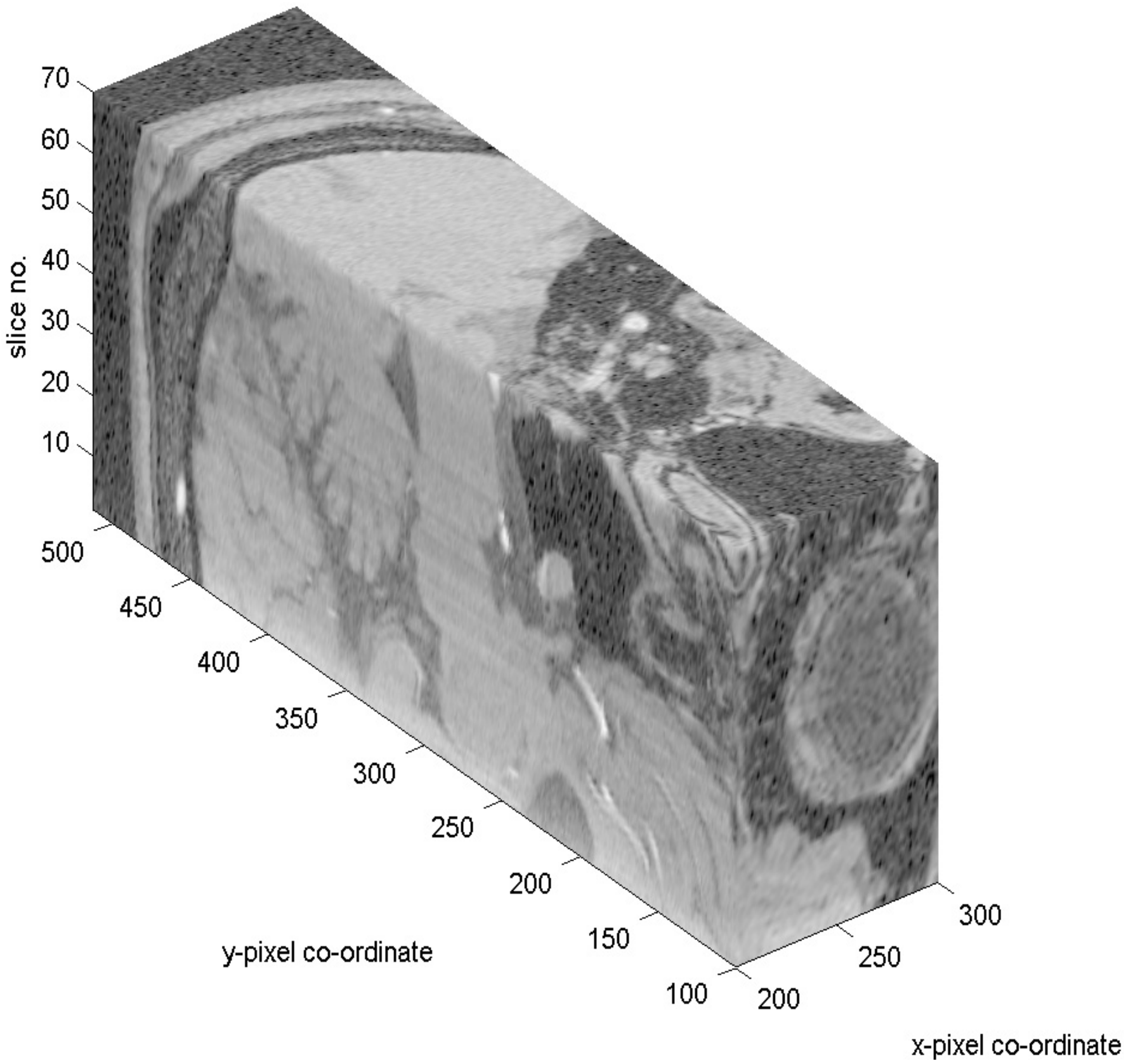

FIGURE 2. Extracted 3-D model of the brain and its visualization rendered as a 3-D view of the stack of images

Time-Frequency Analysis

Time-frequency analysis plays a central role in signal analysis. The Fourier Transform (FT) is only suitable for stationary signals, i.e., signals whose frequency content does not change with time. Fourier analysis is not well suited to describing local changes in frequency content because the frequency components defined by the Fourier transform have infinite (i.e. global) time support.

Discrete Fourier Transform

Discrete Fourier transform (DFT) plays a central role in the implementation of many signal and image processing algorithms. DFT is a mathematical transform which resolves a time series $x(n)$ into the sum of an average component and a series of sinusoids with different amplitudes and frequencies. The N-point DFT, $X(k)$, of an N-point discrete-time sequence, $x(n)$, is defined as

$$X(k) = \sum_{n=0}^{N-1} x(n)\, e^{-j2\pi kn/N} \tag{1}$$

for $k = 0, 1, \ldots, N-1$. The inverse of the DFT is defined as:

$$x(n) = \frac{1}{N} \sum_{k=0}^{N-1} X(k)\, e^{j2\pi kn/N} \quad n = 0, 1, \ldots, N-1 \tag{2}$$

From Eq. (1) it can be seen that the computation of $X(k)$ requires N^2 complex multiplications, thus the DFT is an $O(N^2)$ process. An algorithm was developed by Tukey and Cooley in 1965 called Fast Fourier Transform (FFT) [2] that speeds up the process by computing the DFT using $O(N \log N)$ operations.

Two-dimensional discrete Fourier transform is used for the processing of images. Basis functions are sinusoids with frequency u in one direction times sinusoids with frequency v in the other. For an $M \times N$ image $f[m, n]$, these basis functions can be replaced for computational purposes by complex exponentials $e^{i2\pi um/M}$ and $e^{i2\pi vn/N}$ to evaluate the discrete Fourier transform. The 2-D DFT for an $M \times N$ is usually defined as:

$$F(u, v) = \sum_{m=0}^{M-1} \sum_{n=0}^{N-1} f(m, n)\, e^{-i2\pi(um/M\, +\, vn/N)} \tag{3}$$

and its inverse transform is

$$f(m, n) = \frac{1}{MN} \sum_{u=0}^{M-1} \sum_{v=0}^{N-1} F(u, v)\, e^{i2\pi(um\, +\, vn)} \tag{4}$$

where $F[u, v]$ is the spectrum of the image in the frequency domain and $m = 0, 1, \ldots, M-1, n = 0, 1, \ldots, N-1, u = 0, 1, \ldots, M-1, v = 0, 1, \ldots, N-1$ are all discrete variables.

Filtering may be achieved in the transform domain by first computing the DFT, applying a filter which modifies the transform values, and then applying an inverse transform. The image $f(x, y)$ is first transformed to give $F(u, v)$ and finally the transform is modified using the equation below

$$G(u, v) = H(u, v)\ F(u, v)$$

where $H(u, v)$ is the filter function. The filtered transformed is then inverse-transformed to give the filtered image $g(x, y)$. An illustration of this application is represented in Fig. 3.

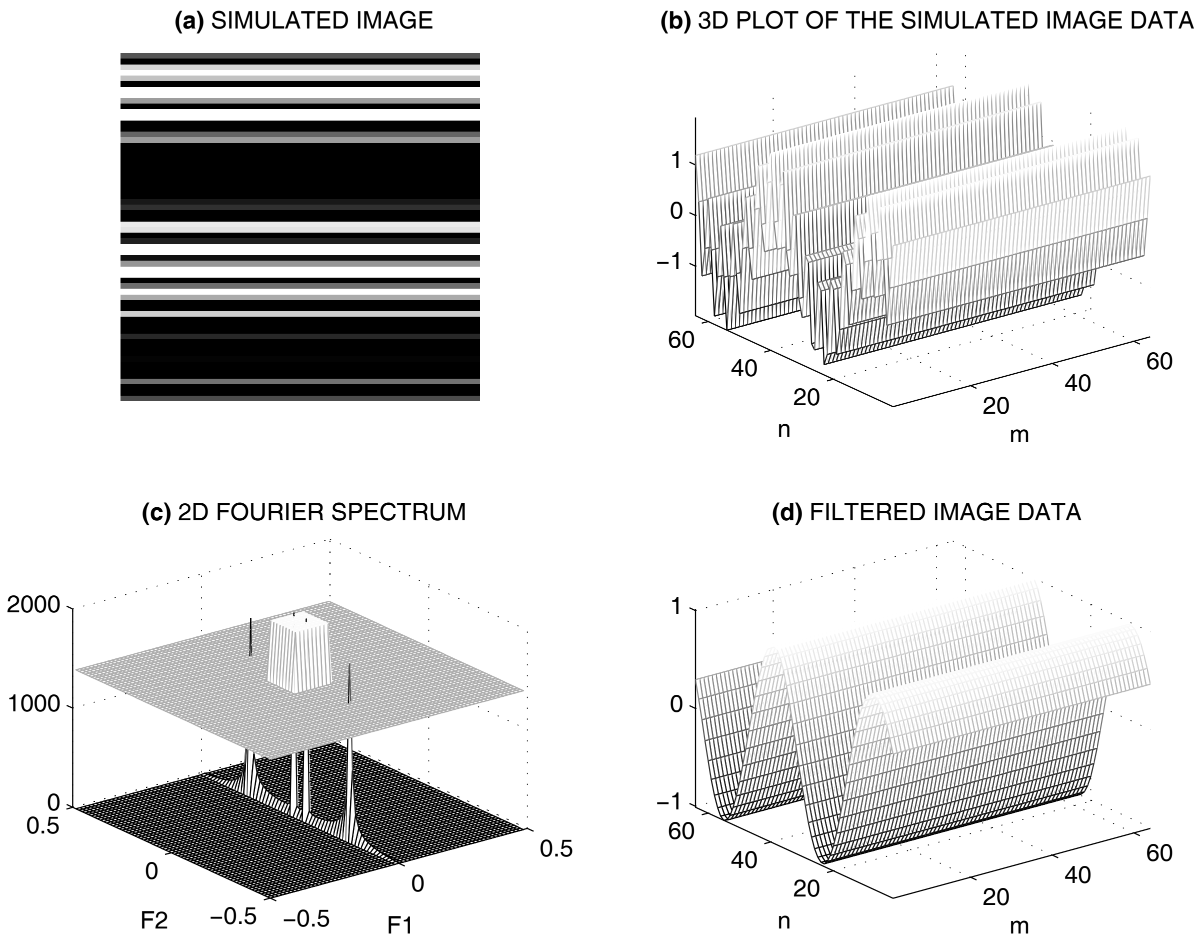

FIGURE 3. Application of the 2-D DFT for the frequency domain filtering presenting (a) simulated image, (b) three-dimensional plot of the image data, (c) DFT of both the two-dimensional signal and the box filter function, and (d) low frequency image data in time domain obtained from the inverse DFT. Scalar product of the filter and signal in frequency domain stand for convolution in time domain

Time-Scale Analysis

The Continuous Wavelet Transform (CWT) provides a time-scale description similar to that of the short time Fourier transform (STFT) with a few important differences: frequency is related to scale and the CWT is able to resolve both time and scale (frequency) events better than the STFT. Wavelet series are thus constructed with two parameters scale and translation, these parameters make it possible to analyze a signal behavior at a dense set of time locations and with respect to a vast range of scales, thus providing the ability to zoom in on the transient behavior of the signal. The CWT [15] is defined as the convolution of $x(t)$ with a wavelet function, $W(t)$, shifted in time by a translation parameter b and a dilation parameter a (Eq. (5))

$$X_W(a,b) = \frac{1}{\sqrt{a}} \int_{-\infty}^{\infty} W\left(\frac{t-b}{a}\right) x(t)dt \tag{5}$$

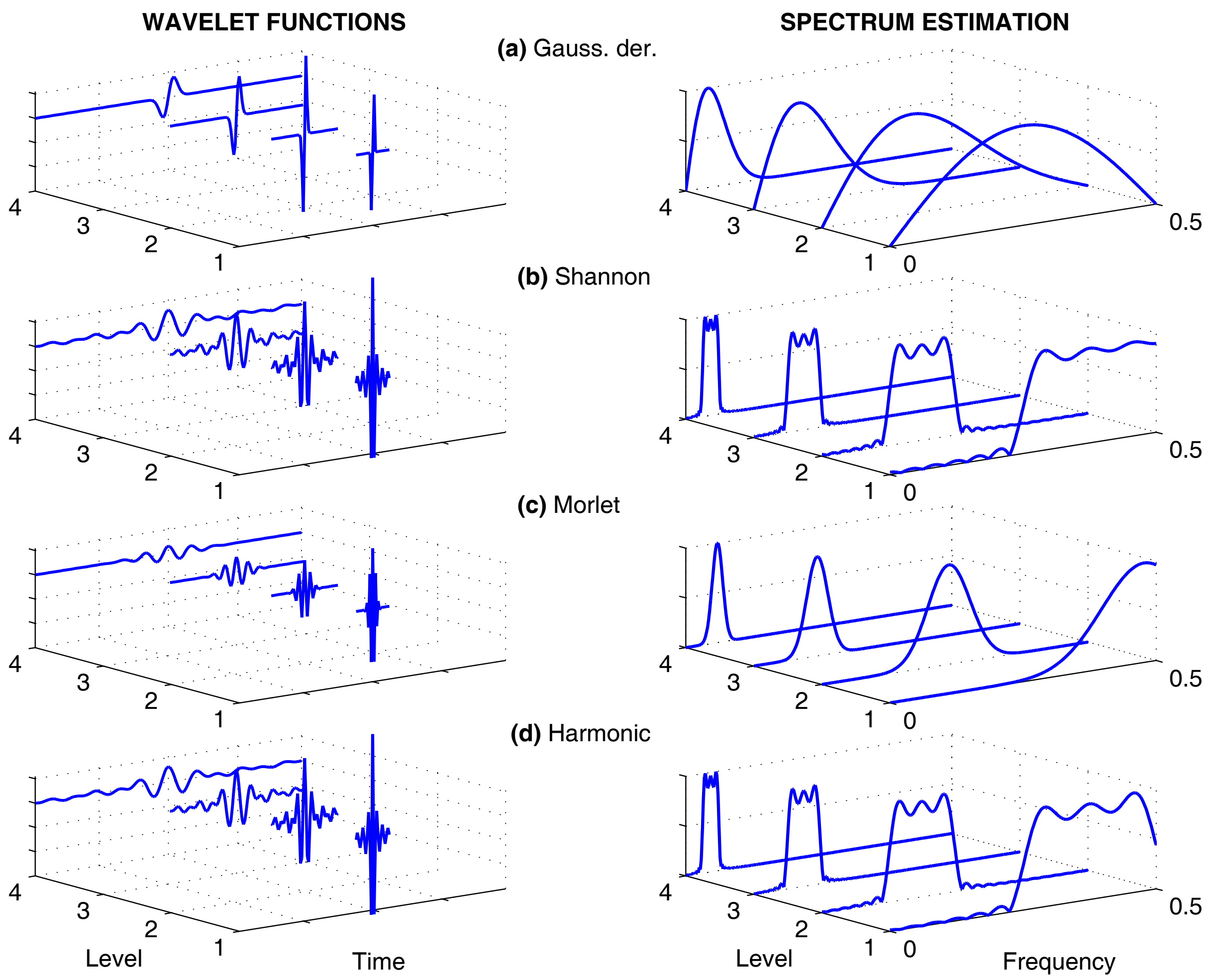

FIGURE 4. Wavelet functions in time and frequency domain

Discrete Wavelet Transform

CWT is redundant since the parameters (a, b) are continuous thus it's necessary to discretize the grid on the time-scale plane corresponding to a discrete set of continuous basis functions. This lead us to a question: how can we discretize the wavelet in Eq. (5)?

$$W_{j,k}(t) = \frac{1}{\sqrt{a_j}} W\left(\frac{t - b_k}{a_j}\right) \tag{6}$$

In theory $a_j = a_0^j$ and $b_k = kb_0a_0^j$ where $j, k \in Z, \quad a_0 > 1, \quad b_0 \neq 0$. The discrete form of the wavelet is shown in Eq. (6), where j controls the dilation and k controls the translation. Two popular choices for the discrete wavelet parameters a_0 and b_0 are 2 and 1 respectively, a configuration that is known as the *dyadic grid* arrangement, Eq. (6) can be written as

$$\begin{aligned} W_{j,k}(t) &= a_0^{-j/2}.\, W(a_0^{-j}\, t - kb_0) \\ &= 2^{-j/2}.\, W(2^{-j}\, t - k) \end{aligned}$$

Wavelet analysis is simply the process of decomposing a signal into shifted and scaled versions of a mother (initial) wavelet. An important property of wavelet analysis is perfect reconstruction, which is the process of reassembling a decomposed signal or image into its original form without loss of information. For decomposition and reconstruction two types of basis functions normally used are:

- Scaling function $\Phi_{jk}(t)$

$$\Phi_{jk}(t) = 2^{-\frac{j}{2}}\, \Phi_0(2^{-j}\, t - k) \tag{7}$$

- Wavelet $W_{jk}(t)$

$$W_{jk}(t) = 2^{-\frac{j}{2}}\, \Psi_0(2^{-j}\, t - k) \tag{8}$$

where m stands for dilation or compression and k is the translation index. Every basis function W is orthogonal to every basis function Φ. An example of a simple wavelet function is called the Haar wavelet. The Haar mother wavelet $W(t)$ and scaling function $\Phi(t)$ are defined as follows:

$$\Phi(t) = \begin{cases} 1 & 0 \leq t \leq 1 \\ 0 & \text{otherwise} \end{cases}$$

$$W(t) = \begin{cases} 1 & 0 \leq t \leq \frac{1}{2} \\ -1 & \frac{1}{2} \leq t \leq 1 \\ 0 & \text{otherwise} \end{cases}$$

Wavelets are functions defined over a finite interval and have an average value of zero.

The 1-D forward wavelet transform of a discrete-time signal $x(n)$ $(n = 0, 1, \ldots, N)$ is performed by convolving signal $x(n)$ with both a half-band low-pass filter L and high-pass filter H and downsampling by two.

$$c(n) = \sum_{n=0}^{L-1} h_0(k)\, x(n-k) \qquad d(n) = \sum_{n=0}^{L-1} h_1(k)\, x(n-k) \tag{9}$$

where $c(n)$ represent the approximation coefficients for $n = 0, 1, 2 \ldots, N-1$ and $d(n)$ are the detail coefficients, h_0 and h_1 , are coefficients of the discrete-time filters L and H respectively

$$\{h_0(n)\}_{n=0}^{L-1} = (h_0(0),\ h_0(1),\ \ldots,\ h_0(L-1))$$

$$\{h_1(n)\}_{n=0}^{L-1} = (h_1(0),\ h_1(1),\ \ldots,\ h_1(L-1))$$

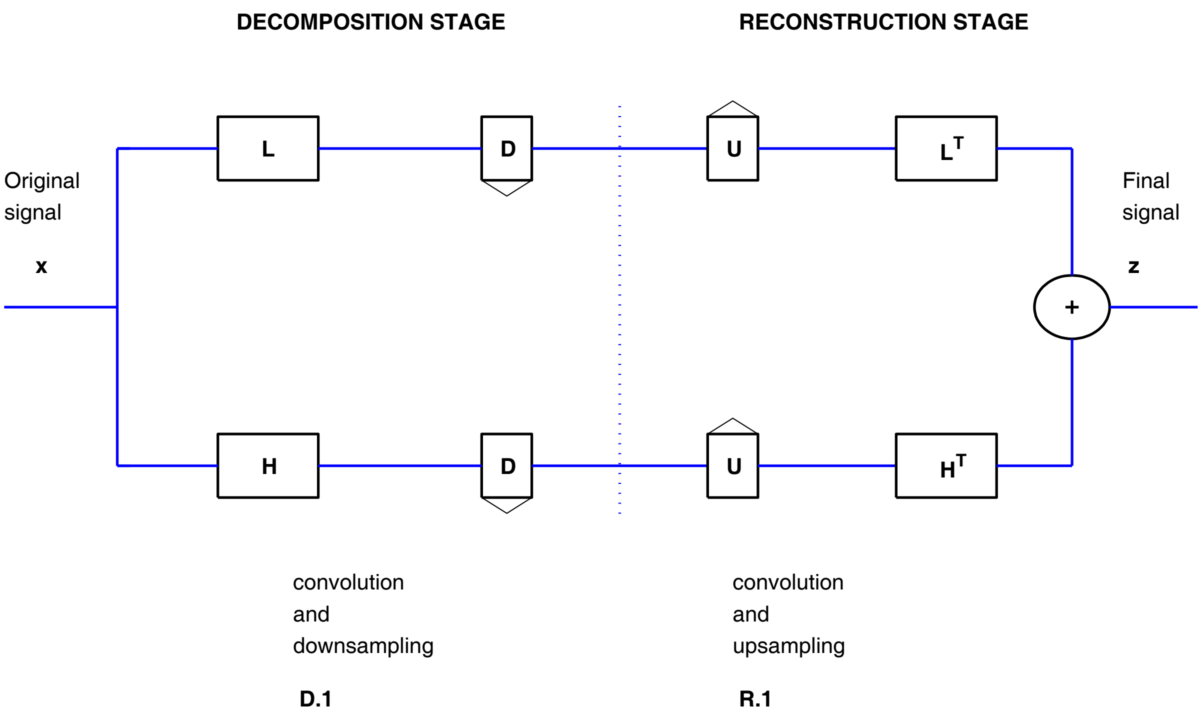

FIGURE 5. Signal decomposition and reconstruction

In Fig. 5, L and H represent the scaling function and wavelet function respectively. A pair of filters: a low-pass filter L and a high-pass filter H, split a signal's bandwidth in two halves. This provides the coefficients $c_j(k)$ and $d_j(k)$ for the decomposition of the signal into its scaling function and wavelet function components. The inverse discrete wavelet transform (IDWT) reconstructs a signal from the approximation and detail coefficients derived from decomposition. The right side of Fig. 5 shows an example of reconstruction.

Two-dimensional Discrete Wavelet Transform

Digital images are 2-D signals that require a two-dimensional wavelet transform. The 2-D DWT analyzes an image across rows and columns in such a way as to separate horizontal, vertical and diagonal details. In the first stage [22] the rows of an $N \times N$ are filtered using a high pass and low pass filters. In the second stage 1-D convolution of the filters with the columns of the filtered image is applied. Each of the branches in the tree is shown in the Fig. 6 therefore produces an $(N/2) \times (N/2)$ subimage. This leads at each level to 4 different subbands HH, HL, LH and LL . The LL is filtered again to get the next level representation, Fig. 6 summarizes the transform for a one level decomposition.

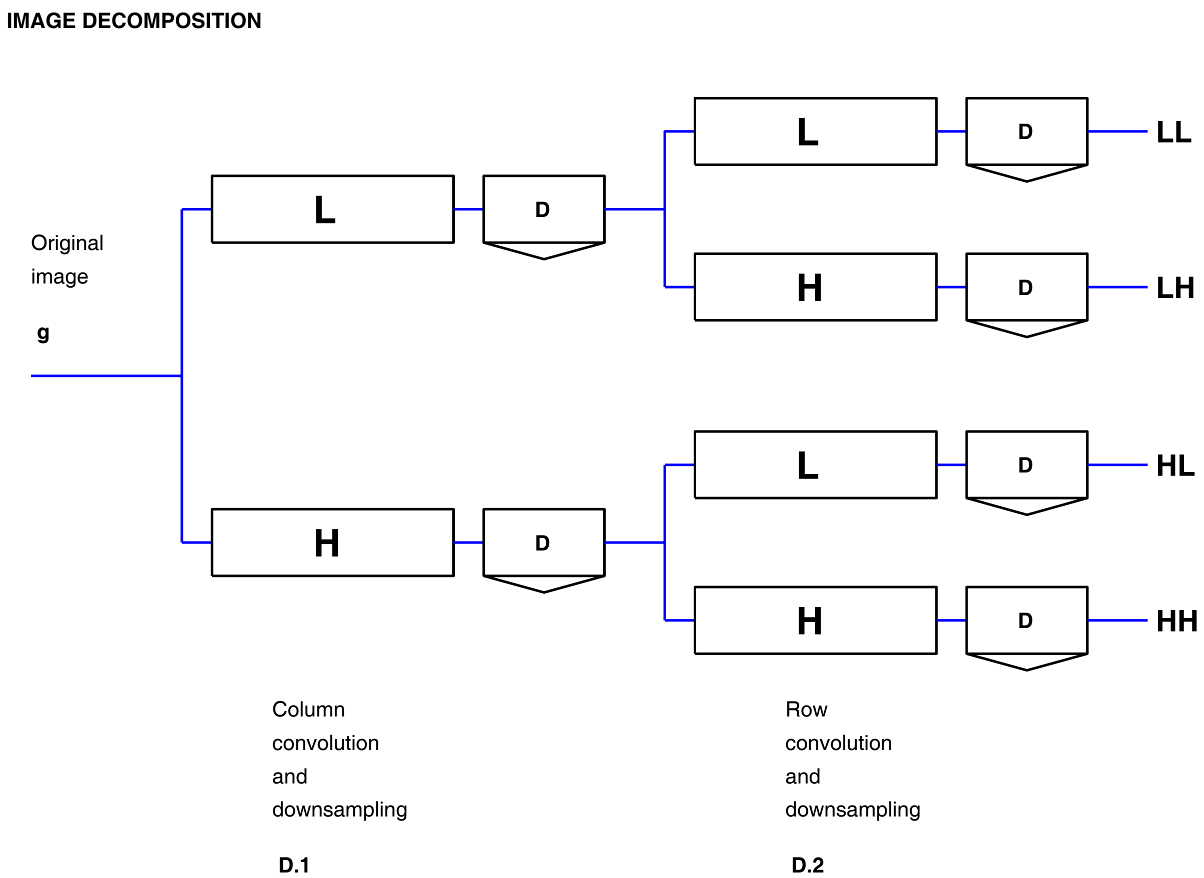

FIGURE 6. A one-level two-dimensional DWT decomposition

To reconstruct the image from its 2-D DWT subimages (LH, HL,HH) the details are recombined with the low pass approximation using upsampling and convolution with the respective synthesis filters. Upsampling refers to the insertion of of a zero row after each existing row or a zero column after each existing column.

Three-dimensional Discrete Wavelet Transform

DWT [19] is a separable, sub-band transform. 3-D wavelets can be constructed as separable products of 1-D wavelets by successively applying a 1-D analyzing wavelet in three spatial directions (x, y, z). Fig. 7 shows a one-level separable 3-D discrete wavelet decomposition [10] of an image volume. The volume $F(x, y, z)$ is firstly filtered along the x-dimension, resulting in a low-pass image $L(x, y, z)$ and a high-pass image $H(x, y, z)$. Both L and H are then filtered along the y-dimension, resulting in four decomposed sub-volumes: LL, LH, HL and HH. Then each of these four subvolumes are filtered along the z-dimension, resulting in eight sub-volumes: *LLL, LLH, LHL, LHH, HLL, HLH, HHL* and *HHH* (Fig 7).

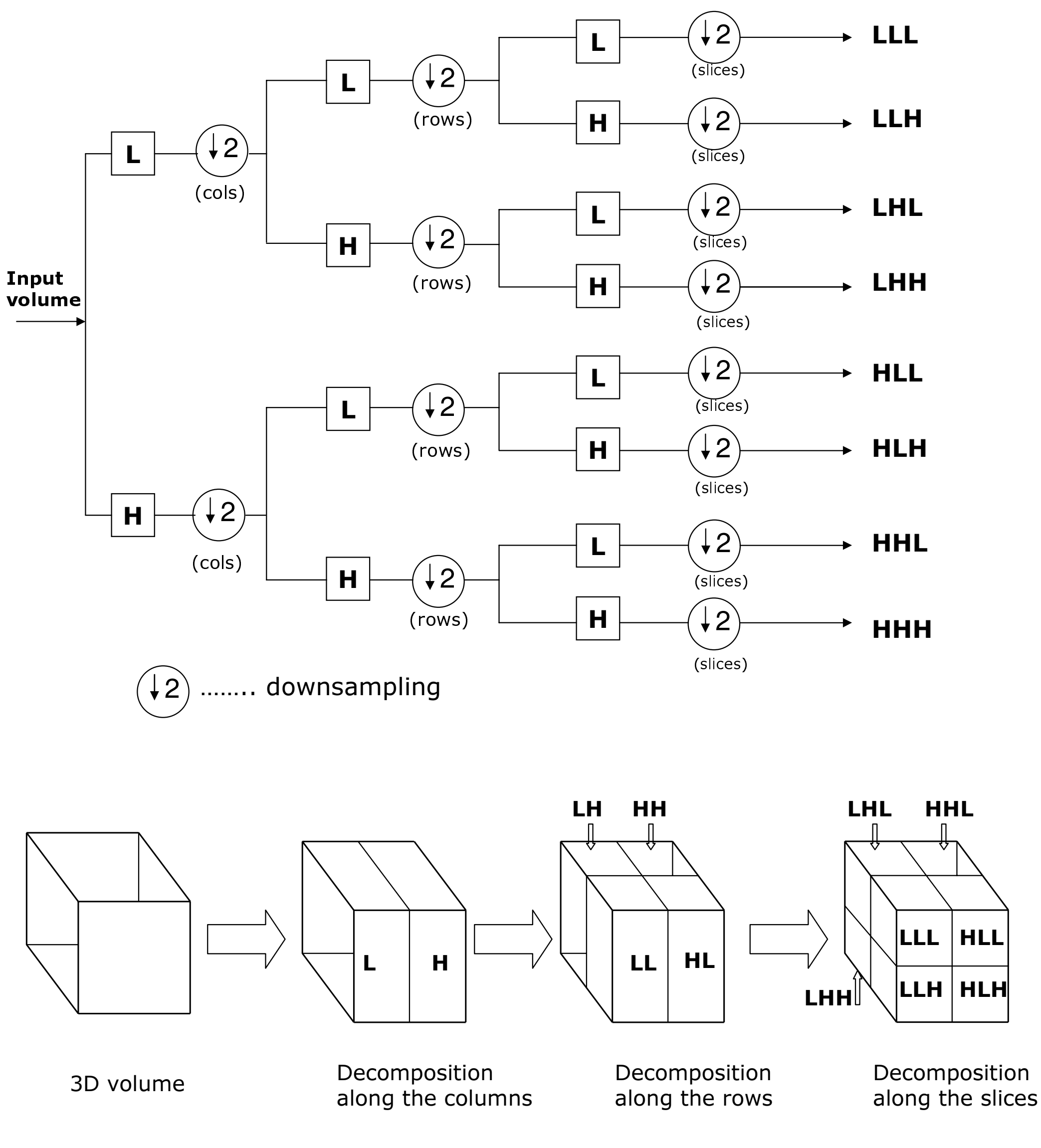

FIGURE 7. Three-dimensional DWT decomposition

Dual Tree Complex Wavelet Transform

Different wavelet techniques can be successfully applied in various signal and image processing methods, namely in image de-noising, segmentation, classification and motion estimation. The thesis discusses the application of dual tree complex wavelet transform (DT CWT) which has significant advantages over real wavelet transform for certain signal processing problems. The transform was proposed by Dr. Nick Kingsbury of Cambridge University. He has written various papers in line to this topic providing a solid mathematical background that allows practical use of complex wavelets in image processing [13, 12, 14, 11].

The 1-D dual-tree wavelet transform [9] is implemented using a pair of filter banks operating on the same data simultaneously. The upper iterated filter bank represents the real part of a complex wavelet transform. The lower one represents the imaginary part.

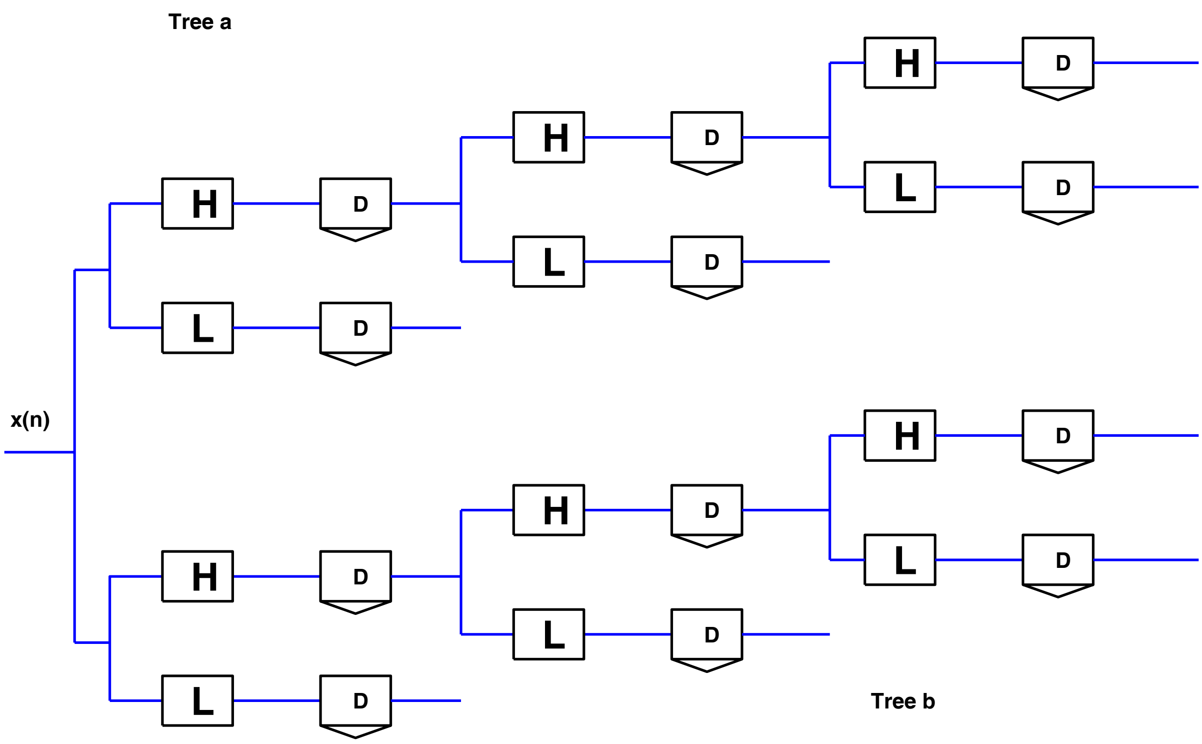

FIGURE 8. The 1-D dual-tree complex wavelet transform .

The shift invariance of 2-D DT CWT is illustrated in Fig. 9, shown are the contributions of the different levels for a circular disk image. Reconstructed images are obtained from the respective details coefficients of the different levels of the DWT and DT CWT. The classical wavelet transform shows aliasing compared to the DT CWT with images which look better and almost free of the aliasing effect.

Fig. 10 illustrates the decomposition of the MR subimage both in the DT CWT and

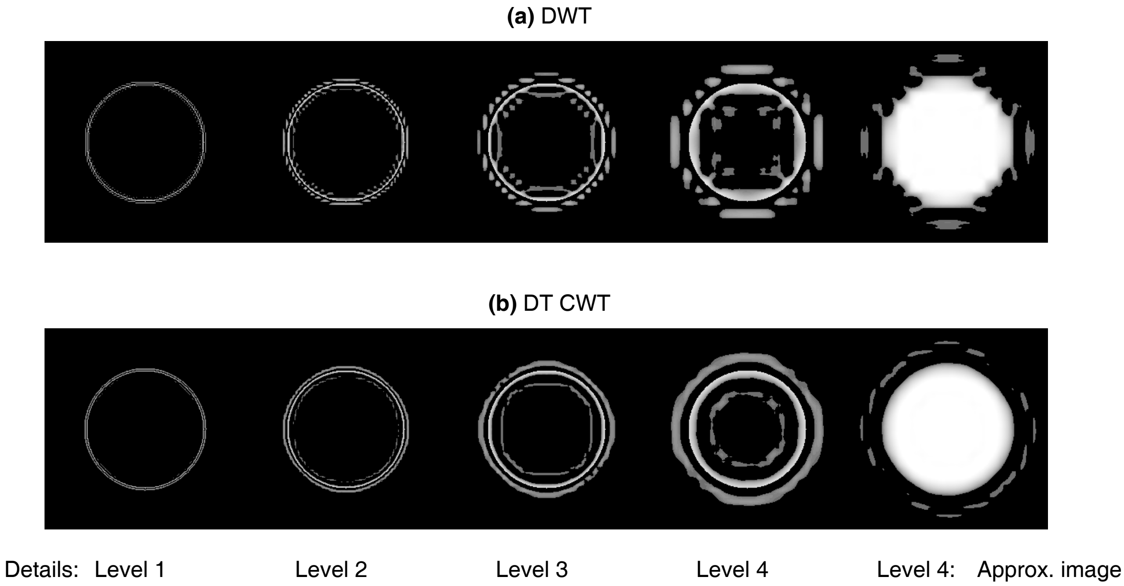

FIGURE 9. Comparison of the shift invariance for (a) DWT and (b) DT CWT

the DWT domain. For each decomposition only two levels are shown and the orientation of the corresponding filter is shown in the corner of each subband. From these figures it is clearly evident that the DT CWT [16] can distinguish the direction in many different orientations compared to the DWT.

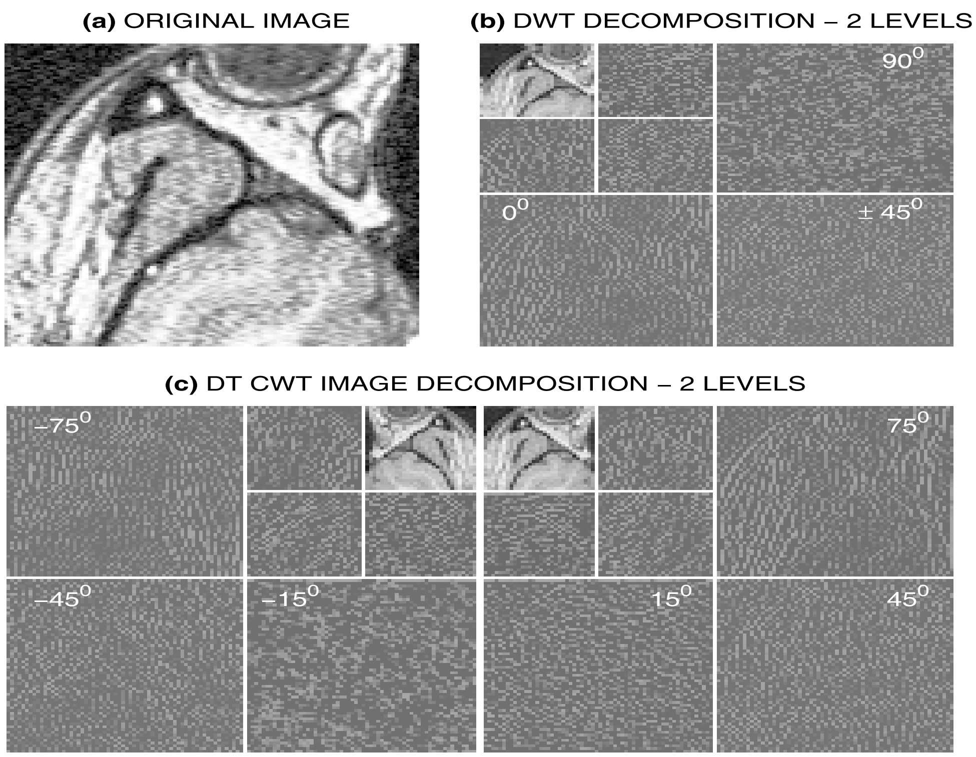

FIGURE 10. Two level decomposition of the (a) original MR image in both, (b) the DWT, and (c) DT CWT domain

Image De-noising

The reduction of noise present in images is an important aspect of image processing. De-noising is a procedure to recover a signal that has been corrupted by noise. After discrete wavelet decomposition the resulting coefficients can be modified to eliminate undesirable signal components. To implement wavelet thresholding a *wavelet shrinkage* method for de-noising the image has been verified. The proposed algorithm to be used is summarized in Algorithm A and it consists of the following steps:

```
Algorithm A: Wavelet image de-noising

  • Choice of a wavelet (e.g. Haar, symmlet, etc) and number of
    levels or scales for the decomposition. Computation of the forward
    wavelet transform of the noisy image.

  • Estimation of a threshold

  • Choice of a shrinkage rule and application of the threshold to the
    detail coefficients. This can be accomplished by hard (Eq. (10))
    or soft thresholding (Eq. (11))

  • Application of the inverse transform (wavelet reconstruction)
    using the modified (thresholded) coefficients
```

Thresholding

Thresholding is a technique used for signal and image de-noising. The shrinkage rule define how we apply the threshold. There are two main approaches which are:

- Hard thresholding deletes all coefficients that are smaller than the threshold λ and keeps the others unchanged. The hard thresholding is defined as follows:

$$\overline{c}_s(k) = \begin{cases} \text{sign } c(k)\ (|\,c(k)\,|) & \text{if } |\,c(k)\,| > \lambda \\ 0 & \text{if } |\,c(k)\,| \leq \lambda \end{cases} \tag{10}$$

  where λ is the threshold and the coefficients that are above the threshold are the only ones to be considered. The coefficients whose absolute values are lower than the threshold are set to zero.

- Soft thresholding deletes the coefficients under the threshold, but scales the ones that are left. The general soft shrinkage rule is defined by:

$$\overline{c}_s(k) = \begin{cases} \text{sign } c(k)\ (|\,c(k)\,| - \lambda) & \text{if } |\,c(k)\,| > \lambda \\ 0 & \text{if } |\,c(k)\,| \leq \lambda \end{cases} \tag{11}$$

Experimental Results

For our test experiments we have considered an additive noise with a uniform distribution which has been used to corrupt our simulated and real MR test image objects. Artificially adding noise to an image allows us to test and assess the performance of various wavelet functions. To reduce computational time a region of interest is cropped (extracted) for the de-noising (Fig. 11).

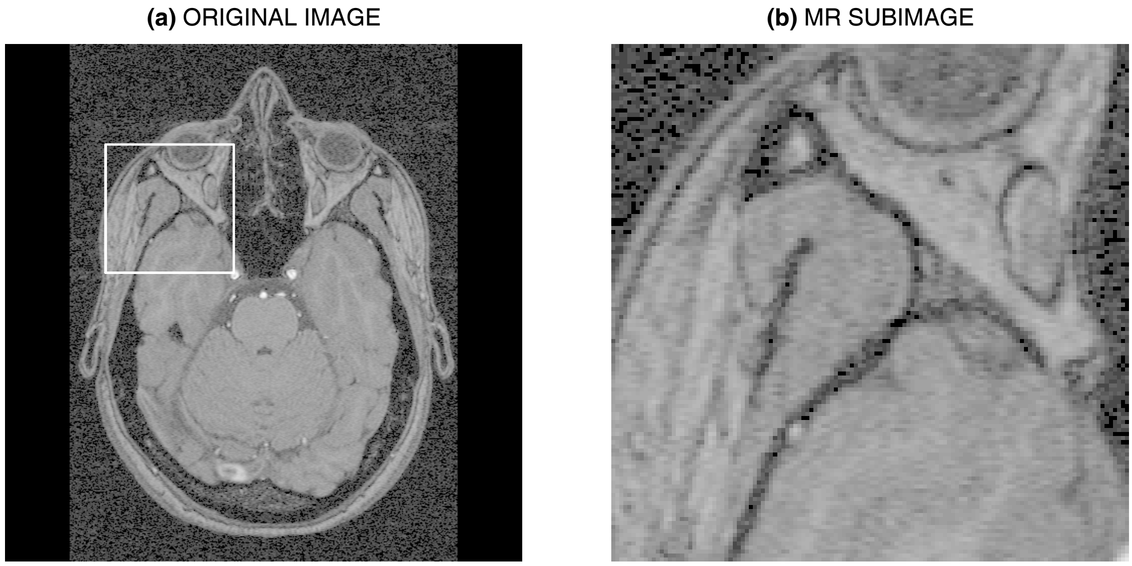

FIGURE 11. Original MR image slice and the chosen subimage for the de-noising application

Algorithm Implementation: We used MATLAB to implement the de-noising algorithm. MATLAB has a wavelet toolbox and functions which are very convenient to do the DWT. A usual way to de-noise is to find a processed image such that it minimizes *mean square error* (MSE), *mean absolute error* (MAE) and increases the value of the *peak signal to noise ratio* (PSNR).

$$MSE = \frac{1}{MN} \sum_{m=0}^{M-1} \sum_{n=0}^{N-1} (y(m,n) - \tilde{y}(m,n))^2 \tag{12}$$

$$PSNR = 10 \log_{10} \left(\frac{I_{max}^2}{MSE} \right) \tag{13}$$

$$MAE = \frac{1}{MN} \sum_{m=0}^{M-1} \sum_{n=0}^{N-1} |y(m,n) - \hat{y}(m,n)| \tag{14}$$

where I_{max} is the maximum intensity of the image, $y(m,n)$ and $\tilde{y}(m,n)$ represent the original image and the de-noised image respectively.

Results from Real MRI Data - 2-D

We have done simulations with uniform random noise added to the MR image. An example of a noisy magnetic resonance image (MRI) which consists of 128×128 pixels is shown in Fig. 12(a). As can be seen in the background the image has been uniformly corrupted with additive noise. The de-noising techniques discussed in the previous section are applied to the noisy MR image to test the efficiency of the different threshold methods.

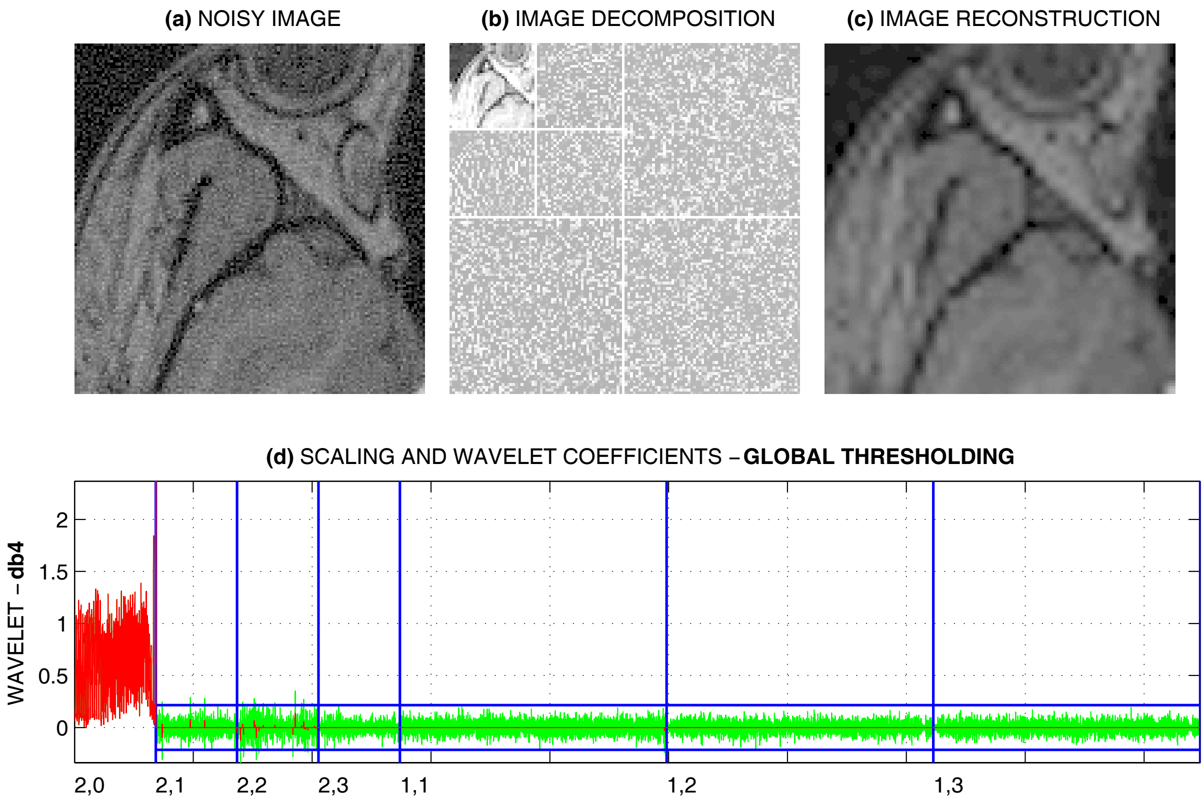

FIGURE 12. The 2-D image decomposition of the (a) noisy MR image using a *db*4 wavelet function, (b) the approximation image (low-frequency component) is in the top-left corner of the transform display, the other subimages contain the high frequency details, (d) global thresholding of the subband coefficients, and (c) shows the resulting de-noised MR image.

TABLE 1. Qualitative analysis (MRI image) - Global thresholding

Type of wavelet	Level 1 MSE	Level 1 MAE	Level 1 PSNR [dB]	Level 2 MSE	Level 2 MAE	Level 2 PSNR [dB]
Noisy image	0.00472	0.29805	23.26	0.00472	0.29805	23.26
Haar	0.00169	0.03245	27.71	0.00157	0.02975	28.04
db2	0.00126	0.02702	28.99	0.00135	0.02789	28.69
db4	**0.00089**	**0.02353**	**30.52**	**0.00115**	**0.02565**	**29.39**
sym2	0.00126	0.02702	28.99	0.00135	0.02789	28.69
sym4	0.00092	0.02334	30.36	0.00119	0.02600	29.24
bior1.1	0.00169	0.03245	27.71	0.00157	0.02975	28.04

Results from Real MRI Data - 3-D

The de-noising algorithm was applied to an MRI sub-volume corrupted with randomly distributed noise. Results from different wavelets are compared using the mean square error (MSE), peak signal-noise-ratio (PSNR) and visual criteria. The MSE is computed relative to the original image volume i.e. it measures the difference between the values of the corresponding pixels from the two volumes. Fig. 13 shows the original MR sub-volume and the noisy volume.

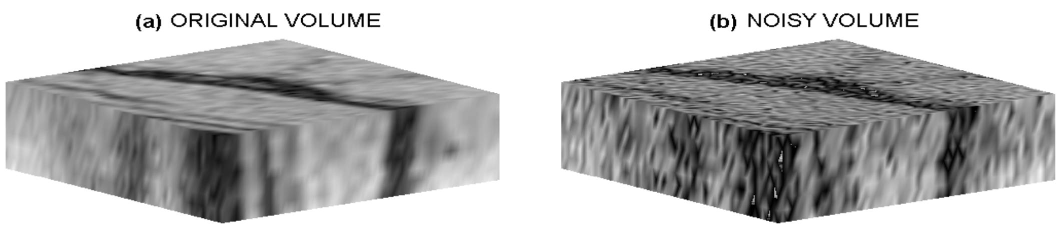

FIGURE 13. Original and noisy MR image volume

We applied 3-D wavelet transform algorithm to an MRI scan of a human brain (128 x 128 x 16). Fig. 14 shows a one level decomposition of the 3-D volume obtained by using the *db*4 wavelet. The ability of the discrete wavelet transform to reduce distortion in the reconstructed volume while retaining all the significant features present in the image volume is seen in Fig. 14(c).

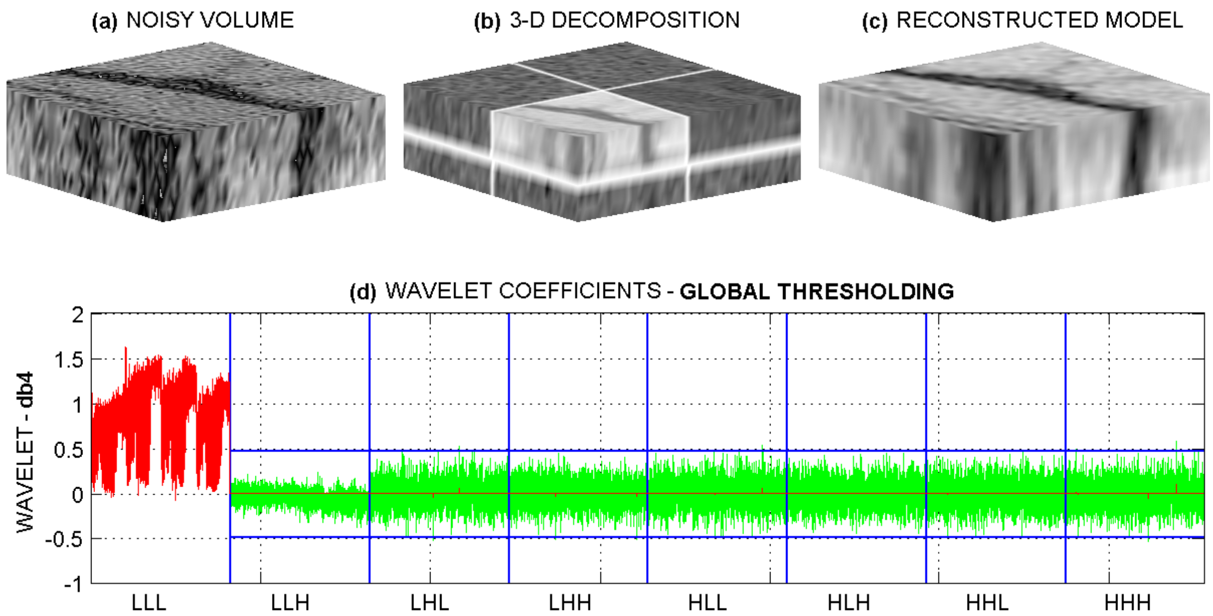

FIGURE 14. Three-dimensional decomposition of (a) noisy MR image volume, (b) one-level image volume decomposition, (c) wavelet coefficients of different subbands (the thresholded values are the ones in red), and (c) the reconstructed model

The proposed 3-D discrete wavelet de-noising algorithm has been evaluated on the noisy MR volume, by visual inspection and by computing quantitative measures of the similarity between the reference image and the de-noised image. The performance of the different wavelets is compared by computing the the error criteria mean square error, mean absolute error and the peak signal-to-noise ratio of the noisy image and the de-noised image. Tables 2, 3 and 4 show the numerical results after the implementation of the global, level-dependent and optimal thresholding respectively. In all the cases the *db*4 wavelet outperforms other wavelets as can be seen from the increase of the PSNR values.

TABLE 2. Qualitative analysis (MRI image volume) - Global thresholding

	Level 1		
Type of wavelet	**MSE**	**MAE**	**PSNR** [dB]
Noisy image	0.01479	0.10096	18.30
Haar	0.00278	0.04145	25.56
db2	0.00322	0.04388	24.92
db4	**0.00216**	**0.03654**	**26.66**
sym2	0.00322	0.04388	24.92
sym4	0.00294	0.04144	25.32
bior1.1	0.00278	0.04145	25.56

TABLE 3. Qualitative analysis (MRI image volume) - Level-dep. thresholding

	Level 1		
Type of wavelet	**MSE**	**MAE**	**PSNR** [dB]
Noisy image	0.01479	0.10096	18.30
Haar	0.00279	0.04149	25.55
db2	0.00324	0.04397	24.89
db4	**0.00216**	**0.03655**	**26.65**
sym2	0.00324	0.04397	24.89
sym4	0.00294	0.04148	25.31
bior1.1	0.00279	0.04149	25.55

TABLE 4. Qualitative analysis (MRI image volume) - Optimal thresholding

	Level 1		
Type of wavelet	**MSE**	**MAE**	**PSNR** [dB]
Noisy image	0.01479	0.10096	18.30
Haar	0.00277	0.04137	25.58
db2	0.00306	0.04329	25.14
db4	**0.00216**	**0.03651**	**26.66**
sym2	0.00306	0.04329	25.14
sym4	0.00280	0.04111	25.53
bior1.1	0.00277	0.04137	25.58

Comparison of the Experimental De-noising Results - DWT and DT CWT

To compare the efficiency of the DT CWT with the classical DWT the quantitative mean square error (MSE) is used. In all cases the optimal thresholds points λ were selected to give the minimum square error from the original image.

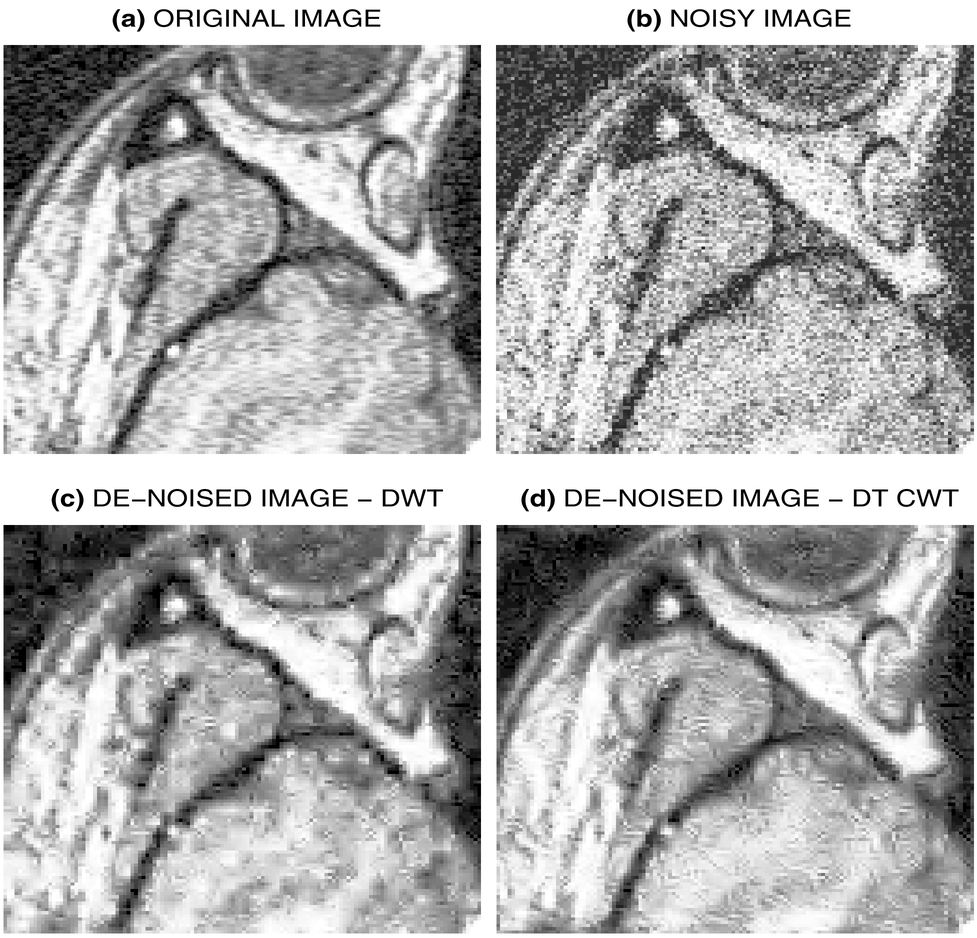

FIGURE 15. MR image scan: (a) original image, (b) with random noise added, (c) de-noised with DWT, and (d) de-noised with dual tree CWT

Experiment results show a great effectiveness of the DT CWT in removing the noise compared to the classical DWT as shown in Tab. 5 by the increase of the $PSNR$ value and the reduction of the MSE.

TABLE 5. Comparison of the 2-D DWT and the 2-D DT CWT de-noising methods

Type of method	Hard thresholding			Soft thresholding		
	MSE	**MAE**	**PSNR** [dB]	**MSE**	**MAE**	**PSNR** [dB]
Noisy image	0.0025	0.0399	25.99	0.0025	0.0399	25.99
DWT	0.0011	0.0257	29.61	0.0009	0.0235	30.46
DT CWT	**0.0009**	**0.0241**	**30.29**	**0.0008**	**0.0226**	**30.81**

Segmentation Results

A watershed algorithm [23] is implemented for the segmentation of artificial texture image and real MR knee image. An *immersion* based approach is adopted to calculate the watershed lines for the segmentation. The principle of this algorithm is simply described in Algorithm B.

```
Algorithm B: Watershed by immersion

  • Visualize the image f(x,y) as a topographic surface, with both
    valleys and mountains.

  • Assume that there is a hole in each minima and the surface is
    immersed into a lake.

  • The water will enter through the holes at the minima and flood the
    surface.

  • To avoid the water coming from two different minima to meet, a dam
    is build whenever there would be a merge of the water.

  • Finally, the only thing visible of the surface would be the dams.
    These dam walls are called the watershed lines.
```

Segmentation of an artificial texture image which contains image objects of different shapes is shown in Fig. 16.

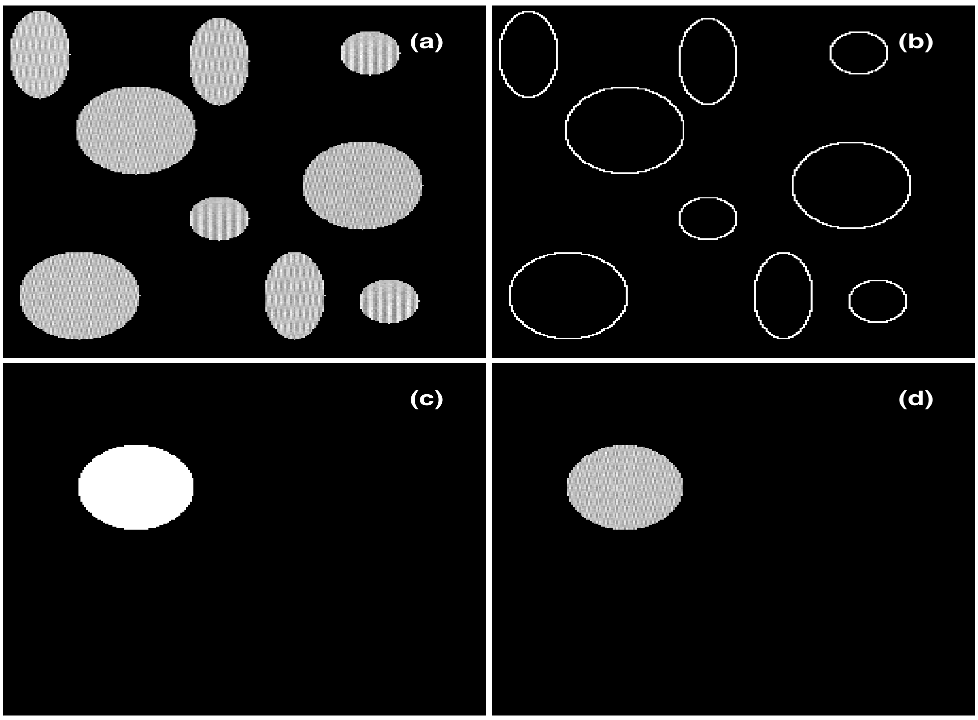

FIGURE 16. Segmentation of (a) simulated image texture, (b) watershed lines, (c) binary image of the selected object, and (d) segmented texture

The most interesting image is the human knee MRI in which three anatomical regions of muscle, bone, tissue and the background of the image are to be segmented. Fig. 17 shows segmentation of bone from MR knee image.

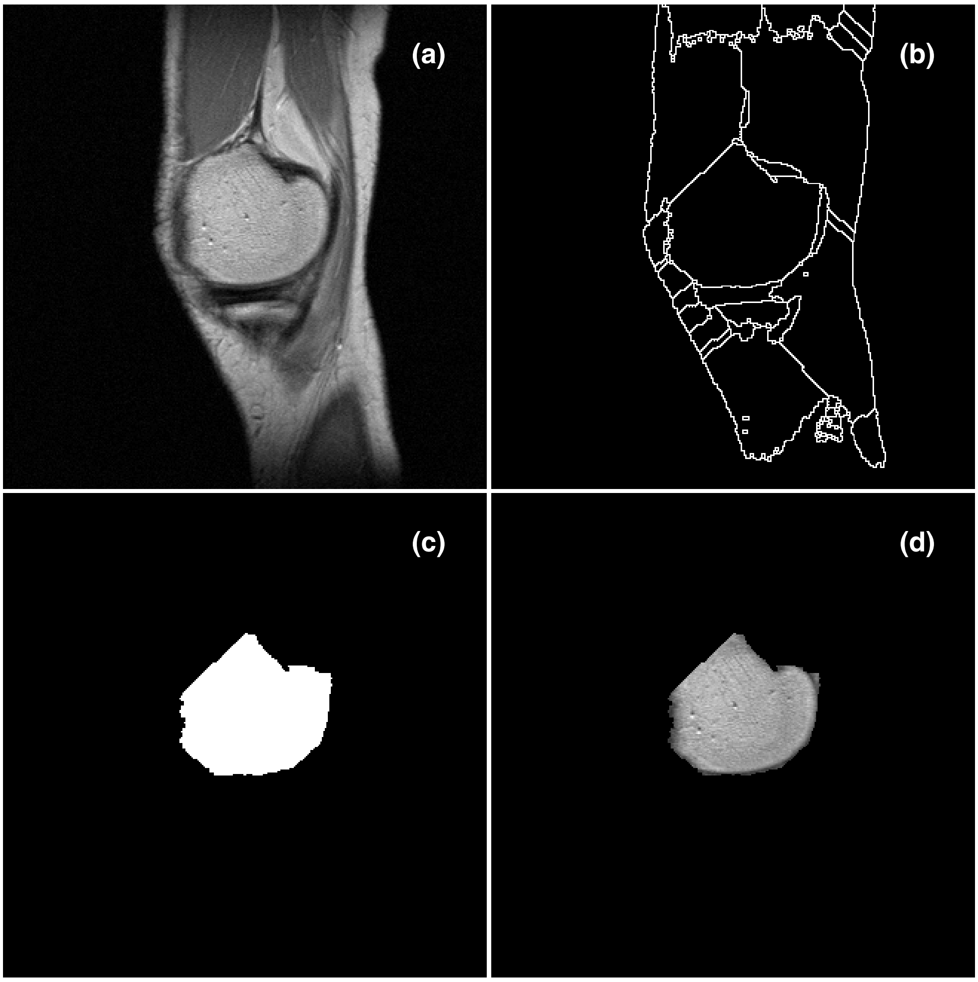

FIGURE 17. Segmentation of the femur in an MR image of the knee. (a) MRI of the knee, (b) watershed lines, (c) binary image of the selected object, and (d) segmented bone

The bone is distinguished from the tissue, the background and the muscle can also be correctly segmented. For clinical application of image analysis, accurate determination of object boundary is often required and such a task is not trivial due to the complexity of biological objects. The watershed-based segmentation of the MR knee image presented here might be useful for expert users to extract object boundary from medical images reproducibly and accurately.

A limitation drawback of the watershed segmentation is that it is sensitive to noise thus resulting in over-segmentation due to an increased number of local minima, such that many catchment basins are subdivided. The first pre-processing would require the reduction of random noise as segmentation results are highly dependent on such type of image noise.

Classification Results of Artificial Image Texture

A competitive neural network is applied for the classification of the simulated image textures shown in Fig. 16(a). In texture classification the goal is to assign an object into one of a predefined set of texture classes. The classification is performed by using a subset of the subband energies that are measured to produce a feature vector that describes the texture. To describe image features a discrete wavelet image decomposition ([4, 20]) using wavelet coefficients at selected levels is applied. The energies of each subimage at selected decomposition levels are used as image features for the classification of the images. The steps involved in extracting the texture feature vector from a grayscale image, are outlined in the following procedure (Algorithm C):

```
Algorithm C: Feature extraction

  • Subject the grayscale image to a chosen level discrete wavelet
    decomposition using the chosen wavelet e.g. the Daubechies wavelet

  • Calculate the energies of the image detail subands.

  • Select any two energies from the detail coefficients to form the
    feature vector
```

The scheme of subband decomposition adopted for the purpose is shown in Fig. 18. For feature extraction only the HH, HL and LH subbands of each stage are considered.

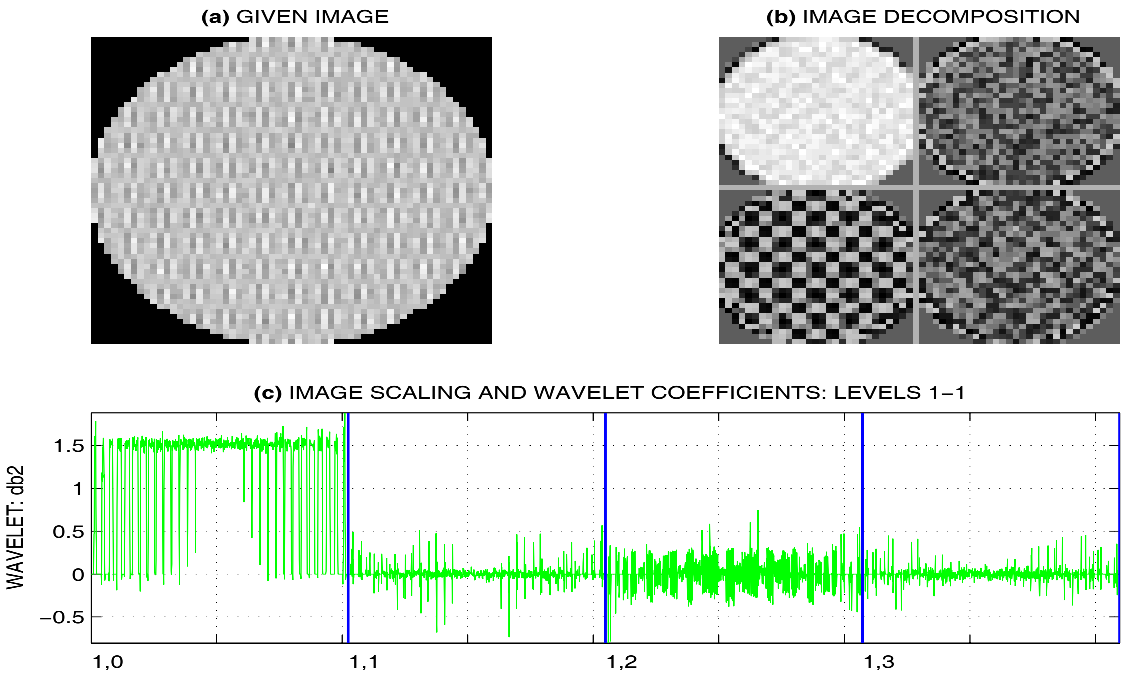

FIGURE 18. One level decomposition of (a) selected image texture, (b) its wavelet decomposition, and (c) the wavelet coefficients

Results of the classification into three classes by a self-organizing neural network are shown in Fig. 19 and Fig. 20 for the feature vectors obtained from the energies of image subband detail coefficients. The feature vectors are obtained from energies of the image detail subbands (horizontal (H), vertical (V) and diagonal (D) detail coefficients) for a chosen decomposition level. The class boundaries are found by setting the biases of the neural network to zero. The boundaries are determined completely by the weights w_{ij} and the biases b_i. Algorithm D below shows how the class boundaries are computed with respect to the Euclidean distance of the the feature vectors and the weights.

```
Algorithm D: Class boundary computation
```

- Find the Euclidian distance between the elements of the pattern matrix and the centre weights

$$d_i = \sqrt{(p_{1k} - w_{i1})^2 + (p_{2k} - w_{i2})^2} + b_i$$

  where $i = 1, 2, \ldots, S$ and $k = 1, 2, \ldots, Q$. S is the number of classes and Q is the number of columns in pattern matrix P.

- Equate each distance to each and every other distances and setting the biases to zero we will get equations of the boundary lines e.g. if $S = 3$ that means $d_1 = d_2$ and $d_1 = d_3$. By equating d_1 to d_2 and expressing p_{1k} as the dependent variable and p_{2k} as the independent variable we will have an equation in the form $p_{1k} = \mathrm{f}(p_{2k})$

$$p_{1k} = \frac{w_{11}^2 + w_{12}^2 - (w_{21}^2 + w_{22})^2 - 2p_{2k}(w_{12} - w_{22})}{2(w_{11} - w_{21})}$$

  This is a linear equation since all the weights are constant except for the variables p_{1k} and p_{2k}. The same applies for other distances i.e. for $d_1 = d_3$ and $d_2 = d_3$.

- Calculate points of intersection for each line with other lines

- Examine the given line segments between all points of intersection - if the middle point of the current segment forms a part of a boundary, the entire segment is a boundary line

- Class boundaries are found in such a way that the two-dimensional plane is divided into the same number of region boundaries as the number of classes

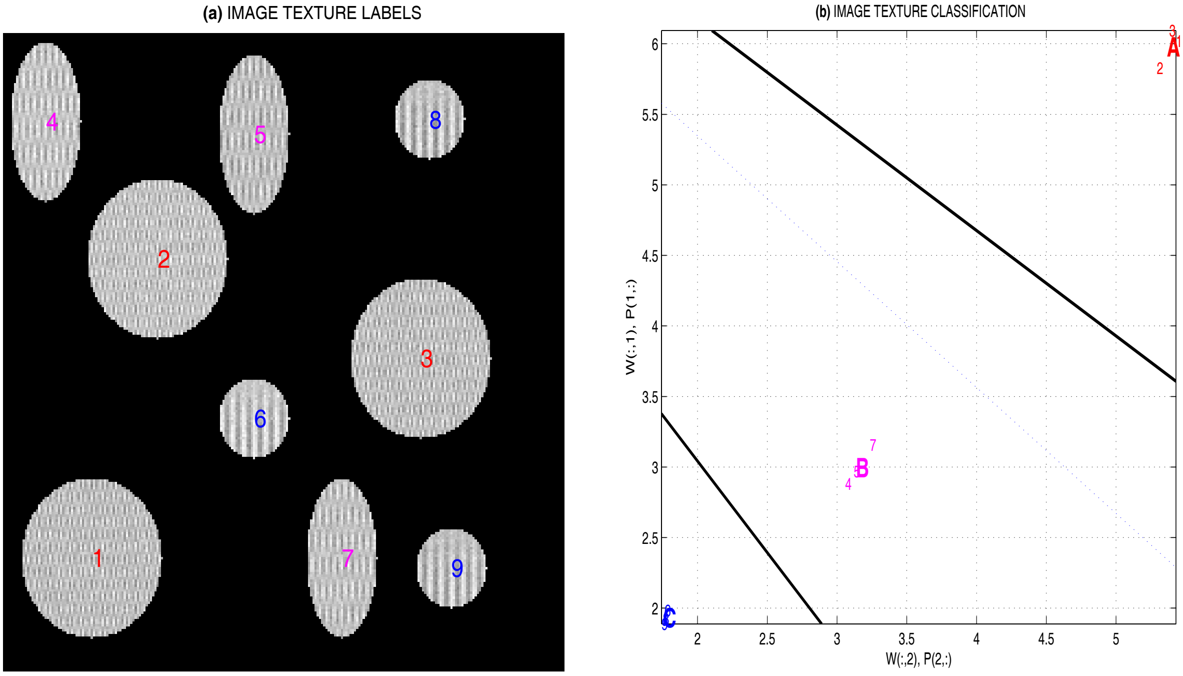

FIGURE 19. Class boundaries and classification of the simulated texture image into three classes. Horizontal (H) and diagonal (D) features from the first level decomposition.

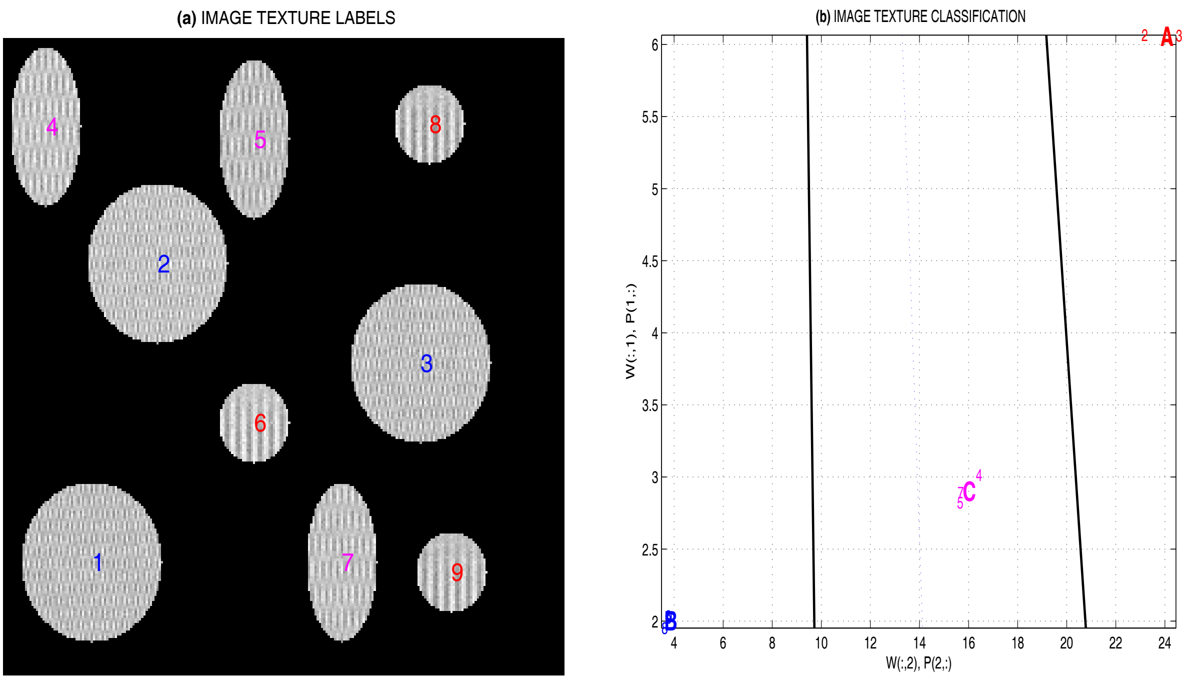

FIGURE 20. Class boundaries and classification of the simulated texture image into three classes. Horizontal (H) and vertical (V) features from the first level decomposition.

Clustering of the image features shows that image textures of similar structure belong to the same class. Fig. 21 presents the texture images typical for individual classes.

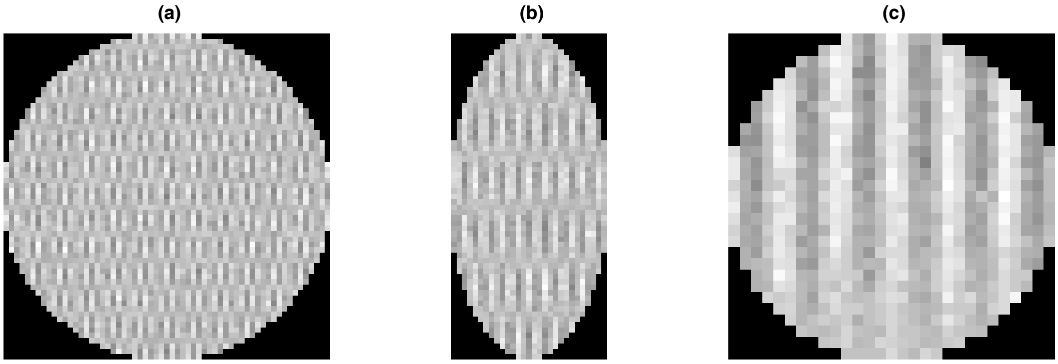

FIGURE 21. Typical image texture of separate classes

Results of texture classification into three classes for different features are compared in Tabs. 6 and 7. Each class is characterized by the variation of signal features distances from the typical class element which resulted from the classification process. It can be observed that features obtained by the discrete wavelet transform based upon different wavelet functions and different number of decomposition levels provide similar results.

TABLE 6. Comparison of image segments classification into three classes using a one level discrete wavelet decomposition (daubechies2 (db2) wavelet function) and taking the horizontal (H), vertical (V) or diagonal (D) coefficients feature source

	Typical Class Image / Number of Images		
	Class Standard Deviation		
Feature	A	B	C
H,D	8/3 0.0214	1/3 0.0460	5/3 0.0789
H,V	6/3 0.0395	1/3 0.2802	7/3 0.1831

TABLE 7. Comparison of image segments classification into three classes using wavelet decomposition into given number of levels (1, 2) by applying the daubechies2 (db2) wavelet function and using the mean (M) and standard deviation (S) feature source

	Typical Class Image / Number of Images		
	Class Standard Deviation		
Feature	A	B	C
1M,1S	6/3 0.0005	4/3 0.0010	1/3 0.0012
1M,2S	3/3 0.0008	9/3 0.0036	4/3 0.0016

Conclusions

The thesis has been devoted to the de-noising algorithms based upon the discrete wavelet transform that can be applied to enhance noisy multidimensional MR data sets i.e. 2-D image slices and 3-D image volumes. The trade-off between noise elimination and detail preservation was analyzed using the MSE, MAE, PSNR and visual criteria. Thus a comparison between the qualities and performance of various wavelet functions were deduced using these criteria. Effectiveness of each filter is dependent on the type of image, the error criterion used, the nature and amount of contaminating noise. It was seen that the fourth-order Daubechies (*db*4) wavelet function performed well for the de-noising of the random noise both in the cases of simulated and real MR data sets, this can be clearly seen with its considerable improvement in PSNR and producing visually more pleasing images. The advantage of the DWT is in its flexibility caused by the choice of various wavelet functions. Since normal random noise constitutes most of the high frequency components by designing a suitable low-pass filter the noise was suppressed to a minimum.

For representing the image data sets, we have used a wavelet transform that is, a multiscale, multiorientation invertible subband representation. The wavelet transform is used to decompose an image into a low-frequency component and a set of higher-frequency details at varying scales of resolution. By analyzing the wavelet transform coefficients, high frequency details which correspond to image noise can be eliminated by using different threshold methods. This way noise is reduced from an image without losing the anatomical information which is of interest to medical doctors. Wavelets have demonstrated to be a very powerful tool for analysis, processing and synthesis of relevant image features.

The implementation of the DT CWT in the de-noising of MR images has been also examined. As shown by the experimental results for most of the de-noising applications the DT CWT gives better results than the classical wavelet transform. Complex wavelets have also proved that they are important tools which can used for other implications of the research such as segmentation and classification. It can be concluded that the DWT and DT CWT are important mathematical tools in biomedical image processing. Finally it is assumed that processing of MR images will result in further methods of image de-noising, edge detection and their enhancement using methods like spline interpolation, resolution enhancement, image reconstruction and feature extraction.

A watershed algorithm for segmentation of MR images was proposed. The principle of the method was described and tested, first, with artificial textures yielding fairly good results. The algorithm was then used to segment a human knee MR image. The anatomical regions: muscle, bone and tissue, and the background could be distinguished. The results show that this method can be comparable to the widely available commercial software, and it performs reasonably well with respect to manual segmentation.

The feature extraction method was computationally efficient in the determination of the feature vectors using coefficients of different subbands. The classification methods studied were neural network methods based on self-organizing network. The methods can be applied for the classification of MR images especially for diagnosis of diseases.

The work presented in this thesis can be extended in several directions. Here we present several of the research directions which might be followed for the further applications in the segmentation and classification of real MR image features rather than the simulated image textures we have used. We review the possible improvements that can be brought to the segmentation algorithms and classification methods proposed in this work.

Efficient texture representation is important for the retrieval of image data. The principle lies in the computation of a small set of of texture describing features for each image in a database so that it is possible to search in the database for images containing a certain feature. DT CWT has been found to be useful for classification as documented in [7].

For clinical application of image analysis, accurate determination of object boundary is often required and such a task is not trivial due to the complexity of biological objects. This thesis presented a watershed-based segmentation algorithm which might be useful for expert users to extract object boundary from medical images reproducibly and accurately. Our on-going research effort is to extend the present algorithm such that it can also distinguish the texture and ultimately incorporate such textural descriptors to real MR brain images for a cooperative boundary or region segmentation framework.

In the thesis we have shown that watershed method provides promising segmentation results which are useful for the segmentation of MR image texture. Better results can be achieved in the case of more precise image segmentation and image pre-processing for noise rejection and artifacts removal. These possibilities can be further extended by the use of complex wavelet functions [7] applied for image decomposition.

Selected results are available from the author's web page: $http://dsp.vscht.cz$

Selected References

[1] A. Bruce, D. Donoho, and Hong-Ye Gao. Wavelet Analysis. *IEEE Spectrum*, 33(10):26–35, October 1996.

[2] J.W. Cooley and J.W. Tukey. An algorithm for the machine calculation of complex fourier series. *Mathematics of Computation*, 19:297–301, 1965.

[3] P. Dastidar. Overview of Neuroradiological MRI . *International Journal of Bioelectromagnetism*, 1(1), 1999.

[4] L. Debnath. *Wavelets and Signal Processing*. Birkhauser Boston, 2003.

[5] F. Fernandes. *Directional, Shift-Insensitive, Complex wavelet Transforms with Controllable Redundancy*. PhD thesis, Rice University, August 2001.

[6] H. Frey, A. Lahtinen, T. Heinonen, and P. Dastidar. Clinical Application of MRI Image Processing in Neurology. *International Journal of Bioelectromagnetism*, 1(1), 1999.

[7] S. Hatipoglu, S. K. Mitra, and N. G. Kingsbury. Texture classification using dual–tree complex wavelet transform. *Image Processing And Its Applications*, (465):344–347, 1999.

[8] T. Heinonen, P. Dastidar, H. Frey, and H. Eskola. Applications of MR Image Segmentation. *International Journal of Bioelectromagnetism*, 1(1), 1999.

[9] A. Jalobeanu, L. Blanc-Feraud, and J. Zerubia. Satellite Image Deconvolution Using Complex Wavelet Packets. Technical report, Institut National de Recherche en Informatique et en Automatique, France, 2000.

[10] H. Khalil and S. Shaheen. Three Dimensional Video Compression. *IEEE Transactions on Image Processing*, 8:762–773, June 1999.

[11] N. Kingsbury and J. Magarey. Motion Estimation Using Complex Wavelets. Technical report, Cambridge University Engineering Department, UK, 1995.

[12] N. G. Kingsbury. The Dual–Tree Complex Wavelet Transform: A New Technique for Shift Invariance and Directional Filters . In *Proceedings of the IEEE Digital Signal Processing Workshop*, 1998.

[13] N. G. Kingsbury. Image Processing with Complex Wavelets. *Phil. Trans. Royal Society London*, 1999.

[14] N. G. Kingsbury and J. F. A. Magarey. Wavelet Transforms in Image Processing. *Proc. First European Conference on Signal Analysis and Prediction*, pages 23–24, June 1997.

[15] Sheng-Tun Li, Shih-Wei Chou, and Jeng-Jong Pan. Multi-resolution spatio-temporal data mining for the study of air pollutant regionalization. In *33rd Annual Hawaii International Conference on System Sciences(HICSS)*, 2000.

[16] P. Loo. *Digital Watermarking Using Complex Wavelets*. PhD thesis, Signal Processing and Communications Laboratory, University of Cambridge, 2002.

[17] L. Najman and M. Couprie. Watershed algorithms and contrast preservation. In *Discrete geometry for computer imagery*, volume 2886 of *Lecture Notes in Computer Science*, pages 62–71. Springer, 2003.

[18] J. Neumann and G. Steidl. Dual–Tree Complex Wavelet Transform in the Frequency Domain and an Application to Signal Classification. *International Journal of Wavelets, Multiresolution and Information Processing IJWMIP*, 2004.

[19] P. Pinnamaneni and J. Meyer. Three-dimensional Wavelet Compression . *2nd Annual Tri-State Engineering Society Meeting*, June 2001.

[20] O. Rioul and M. Vetterli. Wavelets and signal processing. *IEEE Signal Processing Magazine*, pages 14–38, October 1991.

[21] I. W. Selesnick and K. Y. Li. Video denoising using 2d and 3d dual–tree complex wavelet transforms. *Wavelets: Applicationa in Signal and Image Proc. X*, 5207:607–618, August 2003.

[22] J. Van De Vegte. *Fundamentals of Digital Signal Processing*. Prentice Hall, 2001.

[23] L. Vincent and P. Soille. Watersheds in digital spaces: An efficient algorithm based on immersion simulations. *IEEE Transcations Pattern Analysis and Machine Intelligence*, 13(6):583–593, 1991.

List of the Author's Publications

1. A. Procházka, M. Pánek, V. Musoko, M. Mudrová and J. Kukal. Biomedical Image De-noising Using Wavelet Transform. *16th Biennal International EURASIP Conference*, 2002.

2. V. Musoko and A. Procházka. Non-Linear Median Filtering of Biomedical Images. *10th Scientific Conference MATLAB2002*, Humusoft, 2002.

3. V. Musoko, M. Pánek and M. Mudrová. Detection of information carrier signals using band-pass filters. *10th Scientific Conference MATLAB2002*, Humusoft, 2002.

4. V. Musoko and A. Procházka. Three-Dimensional Biomedical Image De-noising. *15th International Conference on Process Control*. STU, Slovakia, 2003.

5. V. Musoko, A. Procházka and A. Pavelka. Implementation of a Matlab Web Server for Internet-based Processing of Biomedical Images. *11th Scientific Conference MATLAB2003*, Humusoft, 2003.

6. J. Kukal, D. Majerová, V. Musoko, A. Procházka and A. Pavelka. Nonlinear Filtering of 3D MRI in MATLAB. *11th Scientific Conference MATLAB2003*, Humusoft, 2003.

7. V. Musoko. Application of Wavelet Transform in Biomedical Image De-noising. *Conference of PhD students*, Faculty of Chemical Engineering, ICT, Prague, 2003.

8. V. Musoko and A. Procházka. Complex Wavelet Transform in Signal and Image Analysis. *14th International Conference on Process Control*. VŠCHT Pardubice, 2004.

9. V. Musoko, M. Kolínová and A. Procházka. Image Classification Using Competitive Neural Networks. *12th Scientific Conference MATLAB2004*, Humusoft, 2004.

10. V. Musoko and A. Procházka. Complex Wavelet Transform in Pattern Recognition. *17th International Conference on Process Control*. STU, Slovakia, 2005.